Research Article

Non-Newtonian fluid flows through backward-facing steps

Houari Ameur[1] · Younes Menni[2]

Abstract

The flows of complex fluids through a backward-facing step are discussed in this paper. The investigation is carried out by means of numerical simulation and using the calculation code Ansys CFX 18.0. The simulated fluids are incompressible and have a non-Newtonian (shear-thinning) behavior modeled by the Oswald's law. The basis of the numerical approach used is the finite volume method. In order to ensure an adequate prediction of the nature of the downstream flows, some results are compared with the experimental measurements and a good agreement is obtained. The study is performed for different geometrical configurations, and for a range of Reynolds number covering the laminar, transitional and turbulent flow regimes, Re is varying from 100 to 12,000. The long-term goals for this study are to explore and actively control the wake dynamics of shear-thinning fluids behind the step which will be useful to determine the wake characteristics behind different types of bodies.

List of symbols

C_f Friction factor (−)
C_p Pressure coefficient (−)
D_h Hydraulic diameter (m)
H Duct height after the step (m)
h Duct height before the step (m)
K Turbulent kinetic energy (J)
ER   Expansion ratio (= S/H)
Re   Reynolds number (−)
S Height of the step (m)
u_0 Inlet velocity (m/s)
W Width of the duct (m)
x, y, z Axial, radial and vertical coordinates, respectively [m]
X_u Reattachment length (m)

Greek letters

μ_a Apparent viscosity (Pa s)
ρ Density (kg/m^3)

1 Introduction

Unstable separated flows have received particular attention due to their presence in many practical applications. Among them, the flow in backward-facing steps, which is representative of several industrial geometries such as weirs, combustion chamber and the sudden enlargement, causes the formation of numerous vortex structures that can play an important role in the phenomena of mixing or combustion [1–7].

The hydrodynamic characteristics of Newtonian fluids have been studied by many researchers [8–11]. Among others, Louda et al. [12] investigated the effect of 3D for the stationary conditions and they reported that these effects have a little importance. The flow through this geometrical configuration is known by its detachment behind the step [13]. The rotating flow backward the step increases the instabilities and interaction between the hot and cold mixed particles of fluid [14]. The combination of the hydrodynamic and thermal instabilities plays

✉ Houari Ameur, houari_ameur@yahoo.fr; ameur@cuniv-naama.dz | [1]Department of Technology, University Centre of Naama (Ctr Univ Naama), PO. Box 66, 45000 Naama, Algeria. [2]Unite of Research on Materials and Renewable Energies – URMER, Department of Physics, Abou Bekr Belkaid University, Tlemcen, Algeria.

an important role on the friction factor (C_f) and Nusselt number (Nu) [14].

Other researchers examined the influence of inclination angle of step [15]. Choi et al. [16] investigated the effect of seven geometrical configurations (10°, 15°, 20°, 25°, 30°, 45° and 90°) for different Reynolds numbers (5000, 8000, 11,000, 15,000, 47,000 and 64,000). They found that the reattachment length remains almost constant for Re > 15,000, even when the inclination angle is increased further than 30°.

With the help of the computational method and for a range of Reynolds number of 36-4500, Macagno and Hung [17] studied the axisymmetric flows of Newtonian fluids through sudden enlargements with an aspect ratio of 2. They reported that the primary task of the eddy for the laminar condition is to shape the flow with a quite low-energy exchange. For a Newtonian fluid flowing through a 1:3 planar symmetric expansion under laminar conditions, Durst et al. [18] observed by experiments two symmetric vortices across the walls of expansion at Re = 56. They observed also the flow bifurcation at Re = 114 with vortices of disparate sizes in both of the prominent corners. For Reynolds number in the range 70–8000, Armaly et al. [9] determined by experiments the velocity distribution and reattachment lengths of a Newtonian fluid through a single backward-facing step. Oliveira and Pinho [19] also explored the flow characteristics of a Newtonian fluid within a backward-facing step, but under laminar flow conditions. For Newtonian fluids, the increase in the expansion ratio may decrease the critical Reynolds number for the symmetry-breaking bifurcation, as reported by Drikakis [20]. At Reynolds number equal to 40.5 and for a 1:3 an axisymmetric abrupt enlargement, Fearn et al. [21] recorded a similar flow bifurcation. For a range of Re from 20 to 211, Hammad et al. [22] studied experimentally the reattachment and redevelopment lengths of a Newtonian fluid flowing through a planar enlargement with an area ratio of 2.

In fact, the fluids flowing via flow devices and through various real-world scenarios are rheologically complex and have a non-Newtonian behavior. Some works have been achieved on this kind of fluids through channels with abrupt enlargement. For the laminar regime and shear-thinning fluids, Mishra and Jayaraman [23] explored by experiments the asymmetric flow patterns through a planar abrupt enlargement with a ratio ER = 16. For power-law fluids and low Re (from 30 to 125), Manica and De Bortoli [24] studied the flow through a 1:3 planar abrupt expansion. They reported that the bifurcation flow for Newtonian fluids occurs at a critical Reynolds number lower than that for the shear-thinning fluids, whereas the shear-thickening fluid shows the least values of critical Re. For low Reynolds number and

power-law fluids with a range of power-law indices from 0.3 to 3, Neofytou [25] used the Casson and power-law models to assess the transformation of symmetric to an asymmetric flow within 1:2 sudden expansion.

Ternik et al. [26] used two models, namely the quadratic viscosity and power-law models, to study the flow of shear-thickening fluids at low Re; they observed a significant effect of the shear-thickening behavior on the flow asymmetry. In another work, Ternik [27] interested in the power-law fluids (with power-law indices from 0.6 to 1.4) at Reynolds numbers from 10^{-4} to 10. They observed a small recirculation, common of creeping flow for the shear-thinning fluids where decreasing the size and strength of the secondary flow. Ameur [28] studied the 3D flows of shear-thinning fluids through sudden expending pipes. He explored the effect of power-law index n (from 0.4 to 1), Reynolds number Re (from 0.1 to 600), spacing between the branching channels, number of branching channels and the expansion ratio. He observed a considerable increase in the pressure losses with the increase in Re and n and decreased expansion ratio. However, he found only a little increase in Δp with decreased spacing ratio, while Δp remained almost the same with increased number of branching channels.

Our search in the literature revealed that the flow of shear-thinning fluids through backward-facing steps for a range of Reynolds number covering the laminar, transitional and turbulent flow regime has not been studied previously. Therefore, the purpose of this paper is to explore the flow patterns of this kind of fluids through a wide range of Re. The Reynolds number is varied between 100 and 12,000.

2 Presentation of the problem

Geometry of the problem studied is a backward-facing step (Fig. 1). Lengths of the ducts before and after the step are $L_1 = 200$ cm and $L_2 = 100$ cm, respectively. These values are sufficient to obtain a developed flow at the entrance region of the duct and to avoid reverse flow at the exit section. Effect of the expansion ratio (ER) is examined by realizing five geometries (ER = S/H = 0.250, 0.375, 0.500, 0.625 and 0.750), where the duct width is taken as $W = 20$ cm. We note here that the side walls of the duct are considered as symmetric, i.e., the problem is treated as two-dimensional, and thus, this value of W has no effect of the flow patterns.

The working fluid is CMC (carboxymethylcellulose) with the following rheological properties: concentration $c = 0.04$ [g CMC/g], consistency index $m = 0.79$ [Pa s^n] and power-law index $n = 0.83$. This fluid has a shear-thinning behavior modeled by the Ostwald model.

Fig. 1 Problem studied
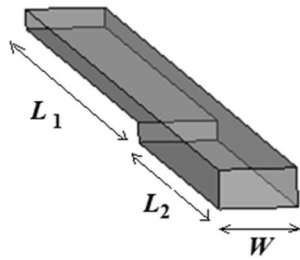
3 Theoretical background

The equations of continuity and momentum for the case studied are given as follows:

$$\frac{\partial}{\partial x_i}\left(\rho u_i\right) = 0 \tag{1}$$

$$\rho\frac{du_i}{dt} = \rho g - \nabla p_i + \mu_a \nabla^2 u_i \tag{2}$$

where μ_a is the apparent viscosity of the non-Newtonian fluid. For a shear-thinning fluid, the Reynolds number is defined as:

$$\mathrm{Re} = \frac{\rho u_0^{2-n} D_h^n}{m}\left(\frac{3n+1}{4n}\right)^{-n} 8^{1-n} \tag{3}$$

where D is the hydraulic diameter, u_0 is the inlet velocity and ρ is the fluid density.

The friction coefficient on the wall permits to determine the point of reattachment flow. It is defined as:

$$C_f(x) = \frac{2}{\mathrm{Re}}\left(\frac{\partial u}{\partial y}\right)_{\mathrm{wall}} \tag{4}$$

In dimensionless form, we define the following parameters:

$$X^* = \frac{x}{H}; Y^* = \frac{y}{H}; Z^* = \frac{z}{H}; S^* = \frac{S}{H} \tag{5}$$

4 Numerical details

The geometry of the computational domain has been created by the CFD software ICEM (Ansys Inc.). Calculations have been achieved with the help of computer tool CFX (version 18.0) which is based on the finite volume method to solve the governing equations. The Reynolds number is varying in a wide range covering the laminar, transitional and turbulent flow regimes. The numerical study is achieved for two-dimensional steady-state, isothermal and
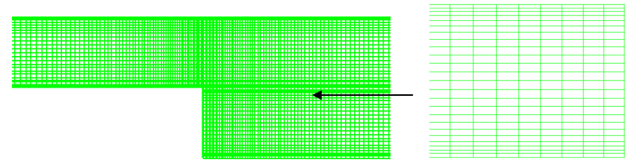

Fig. 2 Computational domain meshed with hexahedral elements

Table 1 Mesh independency tests at $\mathrm{Re} = 7 \times 10^3$

	M1	M2	M3
Number of mesh elements	132,589	869,514	1,558,458
X_u (reattachment length)	5.87105	5.8511	5.8566
Time required [seconds]	45,584	90,856	130,286

incompressible fluid. The second-order upwind scheme was used for the convective terms and the SIMPLEC (Semi-Implicit Method for Pressure-Linked Equations-Consistent) algorithm for the pressure–velocity coupling. The standard $k - \varepsilon$ model is used for the turbulent flow regime. The Boussinesq equation is applied for the flow, with the following boundary conditions: A parabolic profile of velocity is set at the inlet section (Poiseuille), and a Neumann condition is set at the outlet section of duct. At the walls, the no slip boundary condition is set.

Hexahedral grid elements (Fig. 2) were used to discretize the computational domain, and the increased mesh density was created in the downstream region of channel in order to determine the details of the fluid boundary layer. Mesh independency was checked by comparing the converged results of the reattachment length (Table 1). The size function of mesh elements was kept constant during the refinement process, while the size of elements near the walls was reduced. With the mesh of about 0.8 elements, the obtained results of the reattachment length (X_u) did not change by more than 2%. Therefore, this was adopted for further simulations.

With a machine (INTEL® i7 processor with 8 Gb RAM) and for a residual target 10^{-6}, the convergence was achieved after about 3500-4000 iterations, which corresponds to about 25–30 h. CPU time.

5 Results and discussion

5.1 Validation

The accuracy of the predicted results and the correctness of the numerical method have been checked in this section. The experimental works of Hu et al. [29] for a Newtonian fluid and that of Kahine et al. [30] for a shear-thinning fluid have been taken as references for the validation of our numerical results. With the same geometrical configuration and the same fluids as those used by these authors, the results of pressure coefficient and dimensionless axial velocity are presented in Fig. 3a, b, respectively. Furthermore, a comparison between the *k-ε* and the *SST* models against an experimental data of

Hu et al. [29] has been made, as illustrated in Fig. 3a. The comparison between both models and the experimental data of Hu et al. [29] as well as that of Kahine et al. [30] reveals a good agreement. Other researches [31] have used the $k - \varepsilon$ model for the flow through backward-facing steps and they obtained satisfactory results.

5.2 Flow patterns

The backward-facing step (BFS) is a simple and common case to explore the flow behavior. It has been used as a test case to explore the validity and efficiency of numerical methods. In the present geometrical configuration, the fluid is subjected to a sharp expansion where the main flow is separated. A vortex is formed behind the step, where strong adverse pressure gradients and a strong interaction of the different flow structures with the solid wall are present. The dividing streamline from the step tip to the reattachment location X_u defines the shear layer. The line that separates between the primary and secondary recirculation loops is the line that is located between the reattachment and the reseparation points and it is known as the primary–secondary interface line.

Results on the effect of Reynolds number are presented in this section. The streamlines depicted on Fig. 4 illustrate the vortex structure developed behind the step. The important observation in this figure is the presence of a secondary recirculation zone at the top wall of the duct, from Re = 400 (Fig. 4b). With increased Re, the flow on the central axis is intensified and the secondary recirculation zone on the upper wall disappears (Fig. 4c).

For low values of Reynolds number, the flow remained symmetric with a separation location in close proximity of the enlargement corner, the overall size of which is improved with the raise of Re. The increased Re turns the flow into asymmetric, with different separation areas of varying lengths that can be linked to the lower walls of the corresponding conduit.

The critical state is a stability exchange point for the symmetric and axisymmetric conditions. When the value of Reynolds number is sufficiently low, the flow is unable to sustain the disturbance that diminishes via viscous dissipation. The viscous dissipation decreases with increased Re, and the symmetric flow will be altered to stability, as mentioned by Hawa and Ruzak [4].

Even though the BFS is a simple case, it has some fundamental problems that could be transferred into much complicated cases. It is considered to be an optimal geometry for separated flows, due to the wake dynamics in the downstream region of the step.
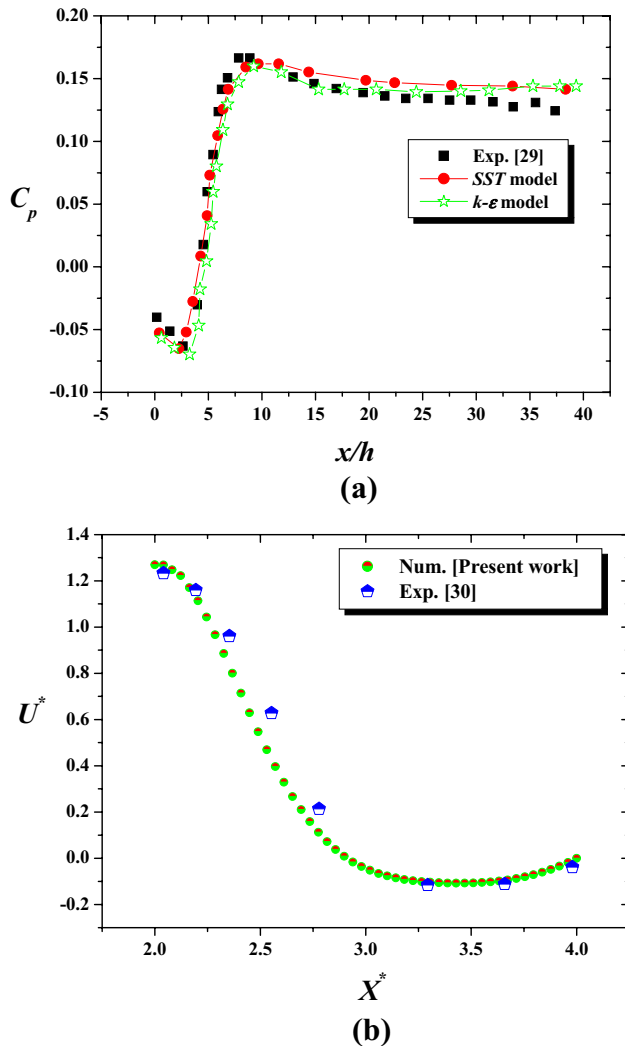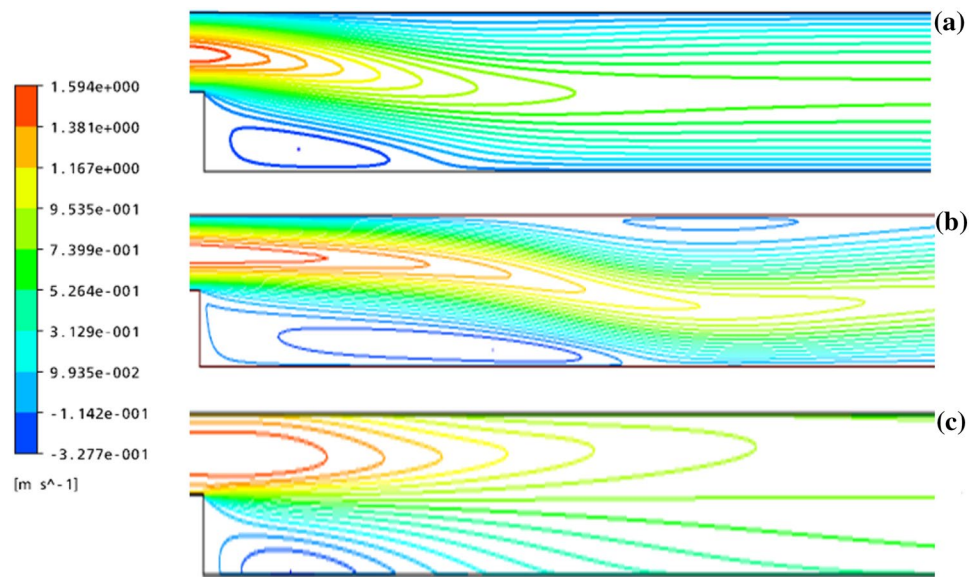

Fig. 3 Validation of our predicted results, **a** pressure coefficient versus dimensionless channel length, **b** axial velocity for $n=0.6$, $d/D=0.112$

Fig. 4 Streamlines for different Reynolds numbers, **a** Re = 100, **b** Re = 400, **c** Re = 3000

5.3 Reattachment length

Our predicted results of the reattachment length vs. Reynolds number have been compared against the experimental data of Armaly et al. [9] and Nie et al. [32] and presented in Fig. 4. We note that the same fluid, as well as the same geometrical configuration as those used by these authors, has been taken in consideration, as detailed bellow. Values of the length (L_1), width (W) and height (h) in the upstream portion of the channel in this section are as follows: 200 cm, 8.0 cm and 0.98 cm, respectively. The values of length (L_2), width (W) and height (h) in the upstream portion of the channel are as follows: 100 cm, 8.0 cm and 1.98 cm, respectively. This geometrical configuration gives a BFS of 1.0 cm in height, an expansion ratio of 2.02:1 and an aspect ratio of 8 at the step. Air has been considered here as a working fluid. As illustrated in Fig. 4, the comparison between our results and those of Armaly et al. [9] and Nie et al. [32] shows a satisfactory agreement.

At the level of expansion, a shear layer generated by the gradient of velocities develops spatially. It interacts with the primary recirculation zone that forms at the bottom wall. This recirculation zone is characterized by an important parameter named reattachment length. Beyond the point of reattachment, the flow tends to develop with a negative pressure gradient. This part of the wall is called the recovery zone. Figure 5 shows the distribution of the reattachment length for the primary recirculation zone as a function of Reynolds number. We note that the numerical values obtained with our computer code show a good agreement with the experimental values of other authors. As the Reynolds number continues to increase, the rate of amplification of instabilities also increases and the intensity of vortex increases. This results in a strong
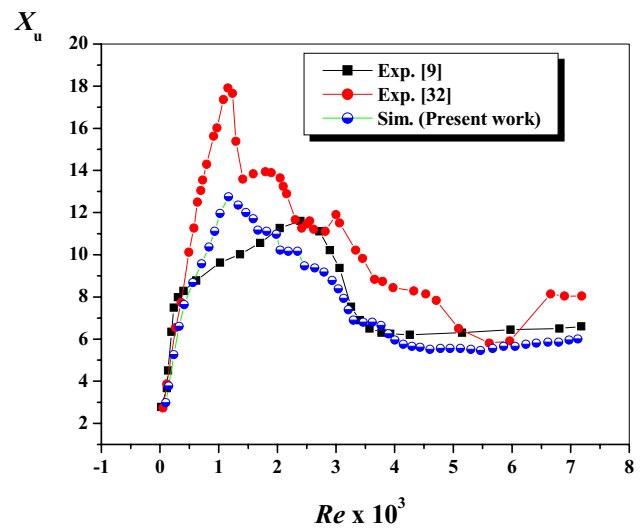

Fig. 5 Reattachment length for different Reynolds numbers

modification of the recirculation zone due to the efficient convective transport of fluid particles to the duct wall. Figure 5 shows that the recirculation length continues to increase up to Re = 1000. For greater Reynolds numbers, the recirculation length decreases, and then, it stabilizes toward Re = 3000 at a value between 5 and 6H. (We remind that X_u = recirculation length/H.)

For the laminar flow conditions (Re between 20 and 211), Hammad et al. [22] observed that the reattachment and redevelopment lengths were generally a linear function of Re. However, the recirculation eddy strength was nonlinear and dependent on Re. They reported also that the recirculation eddy strength becomes weak with the raise of Re.

The separation location in the downstream region behind the step is a single fixed point where the flow separation occurs. The BFS illustrates all important simplifications of several industrial problems with respect to more complicated configurations.

5.4 Axial velocity

Figure 6 describes the flow patterns along the duct. The upstream boundary layer takes off at the top of the step to give rise of the shear layer due to the presence of a strong adverse pressure gradient. The line of separation between the mean flow and the recirculation zone is slightly curved, and the shear layer is thin enough not to be affected by the presence of the wall. In this region, a part of the flow is deflected upstream to generate a recirculation zone, while the other part is redirected downstream with a decreased size of swirling flows.

These structures are intense and visible, especially near the step, and they will be weak further away from the expansion section (Fig. 6).

The expansion ratio (RE) is a measure of the adverse pressure gradient acting on the shear layer as well as a measure of the favorable pressure gradient acting on the recirculation region. A low RE minimizes the effects of the pressure gradient due to expansion (Fig. 7).

5.5 Turbulent kinetic energy

Figure 8 shows the distribution of the turbulent kinetic energy ($K^* = K/\rho u^2$). This energy is defined by the expression $K = 0.5*((u'2) + (v'2) + (w'2))$. It can be seen that the maximum values of turbulent kinetic energy are reached near the step. This is explained by the presence of higher
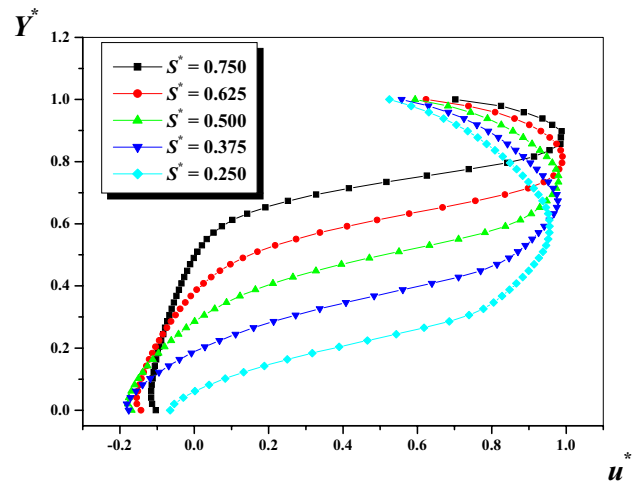

Fig. 7 Axial velocity for Re = 8000, $X^* = 1$, $Z^* = 1$

interaction between the fluid particles just behind the step. Also, the turbulent kinetic energy increases with decreased expansion ratio (Fig. 9).

6 Conclusion

The flow through a backward-facing step (BFS) is characterized by a detachment of the fluid on a sharp edge at 90° and by the formation of vortices downstream of the step. The point of reattachment is the equilibrium position between the vortex and the main flow.

The fluid entrained yields an adverse pressure gradient, thus resulting in the reattachment of the shear layer. The reattachment length, which is considered as one of the
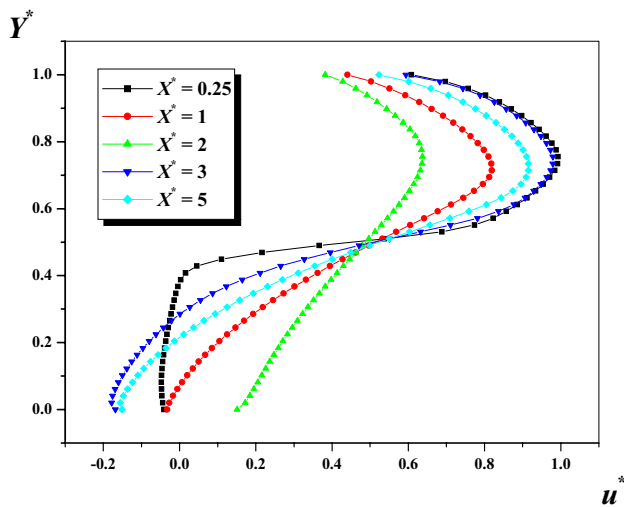

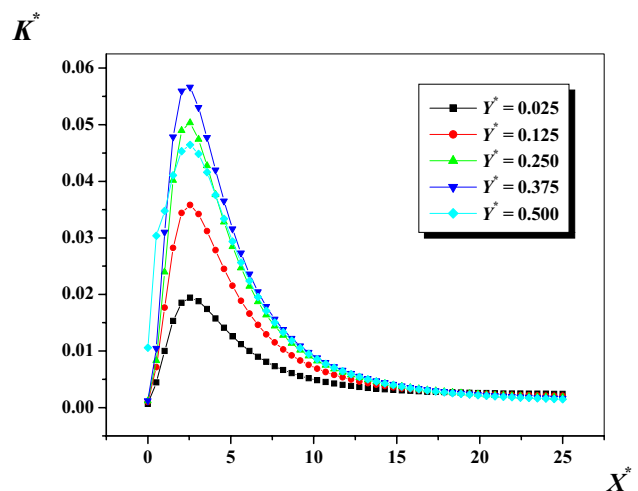**Fig. 6** Axial velocity for Re = 8000, $S^* = 0.5$, $Z^* = 1$

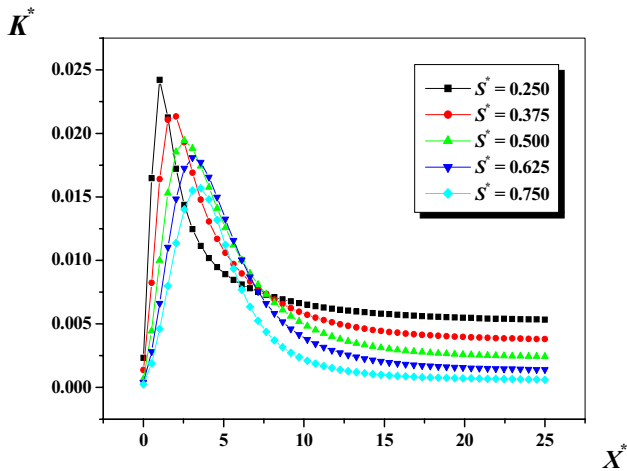**Fig. 8** Turbulent kinetic energy for Re = 12000, $S^* = 0.5$, $Z^* = 1$

Fig. 9 Turbulent kinetic energy for Re = 12000, $Y^* = 0.025$, $Z^* = 1$

primary parameters of the wake characteristics of the BFS flow, is found to be increased in the laminar flow regime and it remained almost constant at the turbulent regime, from Re = 5000.

The vortex size increases and moves downstream as Reynolds number increases in the laminar regime, it decreases and moves upstream for the transient regime, and it decreases or remains almost constant for the turbulent flow. The obtained results show the formation of a secondary vortex at the upper wall for Re = 400, which disappears with increased Re. Finally, the increase in expansion ratio yields a decrease in the turbulent kinetic energy.

Compliance with ethical standards

Conflict of interest The authors declare that they have no conflict of interest.

References

1. Huang W, Li L, Yan L, Liao L (2016) Numerical exploration of mixing and combustion in a dual-mode combustor with backward-facing steps. Acta Astronaut 127:572–578
2. Selimefendigil F, Öztop HF (2017) Forced convection and thermal predictions of pulsating nanofluid flow over a backward facing step with a corrugated bottom wall. Int J Heat Mass Transf 110:231–247
3. Xie WA, Xi GN (2017) Fluid flow and heat transfer characteristics of separation and reattachment flow over a backward-facing step. Int J Ref 74:177–189
4. Hawa T, Rusak Z (2001) The dynamics of a laminar flow in a symmetric channel with a sudden expansion. J Fluid Mech 436:283–320
5. Montazer E, Yarmand H, Salami E, Muhamad MR, Kazi SN, Badarudin A (2018) A brief review study of flow phenomena over a backward-facing step and its optimization. Renew Sustain Energy Rev 82:994–1005
6. Mohammed HA, Fathinia F, Vuthaluru HB, Liu S (2019) CFD based investigations on the effects of blockage shapes on transient mixed convective nanofluid flow over a backward facing step. Powder Technol 346:441–451
7. Nagarajan B, Baraiya NA, Chakravarthy SR (2019) Effect of inlet flow turbulence on the combustion instability in a premixed backward-facing step combustor. Proceed Combust Inst 37:5189–5196
8. Lee T, Mateescu D (1998) Experimental and numerical investigation of 2-D backward-facing step flow. J Fluids Struct 12:703–716
9. Armaly BF, Li A, Nie JH (2003) Measurements in three-dimensional laminar separated flow. Int J Heat Mass Transf 46:3573–3582
10. Wang W, Zhang L, Yan Y (2012) Large eddy simulation of turbulent flow downstream of a backward-facing step. Procedia Eng 31:16–22
11. Pugachev AO, Ravikovich YA, Savin LA (2015) Flow structure in a short chamber of a labyrinth seal with a backward-facing step. Comput Fluids 114:39–47
12. Louda P, Příhoda J, Kozel K, Svácek P (2013) Numerical simulation of flows over 2D and 3D backward-facing inclined steps. Int J Heat Fluid Flow 43:268–276
13. Gautier N, Aider JL (2014) Upstream open loop control of the recirculation area downstream of a backward-facing step. Comptes Rendus Méc 342:382–388
14. Xie WA, Xi GN, Zhong MB (2017) Effect of the vortical structure on heat transfer in the transitional flow over a backward-facing step. Int J Ref 74:465–474
15. Selimefendigil F, Öztop HF (2015) Influence of inclination angle of magnetic field on mixed convection of nanofluid flow over a backward facing step and entropy generation. Adv Powder Technol 26:1663–1675
16. Choi HH, Nguyen VT, Nguyen J (2016) Numerical investigation of backward facing step flow over various step angles. Procedia Eng 154:420–425
17. Macagno EO, Hung T-K (1967) Computational and experimental study of a captive annular eddy. J Fluid Mech 28:43–64
18. Durst F, Melling A, Whitelaw J (1974) Low Reynolds number flow over a plane symmetric sudden expansion. J Fluid Mech 64:111–128
19. Oliveira P, Pinho F (1997) Pressure drop coefficient of laminar Newtonian flow in axisymmetric sudden expansions. Int J Heat Fluid Flow 18:518–529
20. Drikakis D (1997) Bifurcation phenomena in incompressible sudden expansion flows. Phys Fluids 9:76–87
21. Fearn R, Mullin T, Cliffe K (1990) Nonlinear flow phenomena in a symmetric sudden expansion. J Fluid Mech 211:595–608
22. Hammad KJ, Ötügen MV, Arik EB (1999) A PIV study of the laminar axisymmetric sudden expansion flow. Exp Fuids 26:266–272
23. Mishra S, Jayaraman K (2002) Asymmetric flows in planar symmetric channels with large expansion ratio. Int J Numer Methods Fluids 38:945–962
24. Manica R, De Bortoli A (2004) Simulation of sudden expansion flows for power-law fluids. J Non-Newton Fluid Mech 121:35–40
25. Neofytou P (2006) Transition to asymmetry of generalised Newtonian fluid flows through a symmetric sudden expansion. J Non-Newton Fluid Mech 133:132–140
26. Ternik P (2009) Planar sudden symmetric expansion flows and bifurcation phenomena of purely viscous shear-thinning fluids. J Non-Newton Fluid Mech 157:15–25
27. Ternik P (2010) New contributions on laminar flow of inelastic non-Newtonian fluid in the two-dimensional symmetric expansion: creeping and slowly moving flow conditions. J Non-Newton Fluid Mech 165:1400–1411

28. Ameur H (2018) Pressure drop and vortex size of power law fluids flow in branching channels with sudden expansion. J Appl Fluid Mech 11:1739–1749
29. Hu R, Wang L, Fu S (2016) Investigation of the coherent structures in flow behind a backward-facing step. Int J Numer Methods Heat Fluid Flow 26:1050–1068
30. Kahine K, Nguyen VT, Lebouché M (1997) Flow of non-Newtonian fluids in sudden expansions. Int Commun Heat Mass Transf 24:1103–1112 **(In French)**
31. Huang R, Luo X, Ji B, Ji Q (2017) Turbulent flows over a backward facing step simulated using a modified partially averaged Navier–Stokes model. J Fluids Eng 139:044501
32. Nie JH, Armaly BF (2004) Reverse flow regions in three-dimensional backward-facing step flow. Int J Heat Mass Transf 47:4713–4720

Publisher's Note Springer Nature remains neutral with regard to jurisdictional claims in published maps and institutional affiliations.